Master's Thesis

Improved continuous magnetic separation assisted with advection flows in microfluidic channels.

Su Hyun Jung

Department of Biomedical Engineering

Graduate School of UNIST

2019

Improved continuous magnetic separation assisted with advection flows in microfluidic channels.

Su Hyun Jung

Department of Biomedical Engineering

Graduate School of UNIST

Improved continuous magnetic separation assisted with advection flows in microfluidic channels.

A thesis/dissertation
submitted to the Graduate School of UNIST
in partial fulfillment of the
requirements for the degree of
Master of Science

Su Hyun Jung

01. 02. 2019
Approved by

Advisor
Joo Hun Kang

Improved continuous magnetic separation assisted with advection flows in microfluidic channels.

This certifies that the thesis/dissertation of Su Hyun Jung is approved.

01. 02. 2019

Advisor: Joo Hun Kang

박정훈

Jung-Hoon Park: Thesis Committee Member #1

박 태 은

Tae-Eun Park: Thesis Committee Member #2

Abstract

Magnetophoretic separation efficiency is determined by a ratio of magnetic particles isolated by magnetic flux density gradients. Because the magnetic flux density gradients rapidly decrease as the distance from the magnetic source increases, the magetic particles which are placed far from the magnetic source are not separated. This is one of the key challenges to achieve high throughput magnetic separation device. Here, we report a magnetic separation device inducing specific fluid flow by patterning the obstacle arrays on the channel. We achieve highly augmented magnetic separation efficiency using chaotic convection flows induced by the slanted ridges in the channels. The asymmetric pressure gradients across the cross-section of the channel are induced by the slanted ridge arrays pattern in the channel, and then it occurs the spiral flows inside the microchannel. The spiral flows transfer the magnetic particles or biological cells integrated with magnetic particles toward the area with high magnetic flux density gradient where is close to the ferromagnetic nickel structure with magnet. With this suggested approach, over 91.68% of *E. coli* bound with magnetic nanoparticles (200 nm) in whole blood are successfully isolated at a flow rate up to 1.6 mL/h, in a single microfluidic channel, whereas conventional devices without advective rotational flows only isolated under 27.72%.

Contents

List of figures

1. Introduction

Magnetic separation for biological research has been widely used to isolate diverse kinds of targets from the samples[1]. Since microfluidic techniques emerged, many researchers tried to integrate the magnetic source with microfluidic systems to acomplish the substantial high throughput separation of diverse biomolecules from biological sample[2]. The most common approach to improve magnetic separation in a microfluidic device was integration of ferromagnetic microstructures that locally enhance magnetic flux density gradients across the microfluidic channels[3], [4]. Due to its positive features like simplicity, enhanced separation efficiency and variability of objects it could target by utilizing antibody immobilized on the surface of magnetic particles, magnetic separation combined with a microfluidic device has attracted great attention and has demonstrated many promising applications, including separation of tumor cells[5], nucleic acids[6], and pathogens[7], [8]. Despite its utility in a wide range of applications, it has been a daunting task to improve its throughput because the magnetic force sufficient to separate magnetic particles is only available at a distance of less than 100 μm. The shortage of magnetic force becomes the huge limitation to scale up the magnetic separation device for the applicable clinical systems.

To demonstrate magnetic separation in a large scale (>20~50 mL), it has been mostly carried out using 50 mL tubes attached to commercial magnetic separators[50mL tube Magnetic Separator; Thermofisher scientific, USA], and improving its separation efficiency was recently attempted by employing the augmented magnetic flux density gradients[9]. Despite of these efforts, they mainly rely on micrometer-sized magnetic particles due to their large magnetic moments and rapid magnetic separation velocity in a large scale magnetic separator. According to our previous report[10], micrometer-sized magnetic particles might hinder the ability of binding relatively small objects in biological samples, such as bacteria cells in blood. Thus, we need to use nanometer sized (< 500 nm) paramagnetic particles to efficiently capture small biomolecules or cells in complex biological fluids, but magnetic separators isolating nanometer-sized magnetic particles are available only for a small scale (~1 mL) and limited throughputs in a range of 10 mL/hour [7]. To address this, we demonstrated a magnetic separation device patterned with slanted ridge arrays that induce spiral flows, which transfer the magnetic particles in the direction of a magnetic energy source, where the magnetic particles are rapidly isolated by the strong magnetic drag force.

This design give the capability of microfluidic-magnetic separation devices to separate nanometer-sized magnetic particles at higher flow rates even in complex biological samples. Especially, isolation of

target cells from the whole blood is in high demand in terms of the diagnostics and extracorporeal blood cleansing therapy. Whole blood contains various kinds of elements including blood cells, plasma which is fully filled with diverse proteins, and the major effect of these components is forming high viscosity that reduces the magnetic drag velocity to applied for isolating magnetic particles connected with targets. Pretreatment of the whole blood for making easy to load the sample in microfluidic systems has been widely introduced, however, the complex pretreatment steps cause the loss of rare cells from the patient's blood. Moreover, the process of diluting blood is not utilized for the blood cleansing system to cure the patients who are infected by fetal bacteria. Herein, we demonstrate the new approach for the magnetic separation system which can continuously separate the targets form the unprocessed whole blood.

2. Materials and Methods.

2.1 Device fabrication

To embed micro nickel structure in poly(dimethylsiloxane) (PDMS) layer on the slide glass, we cured the PDMS reagent on the nickel structure placed on the slide glass. The PDMS curing reagent and prepolymer were mixed in a ratio of 1 to 10. Before pouring the mixture, air bubbles in mixture were removed by vacuum system to prevent the leakage of device because of the rough PDMS layer surface formed by air bubble. Mixture that had been poured on the nickel structure with slide glass was cured on 65 degree in oven at overnight. By making pressure during curing time, the thin PDMS layer was generated on the slide glass with the thickness of 100 μm[11]. The mold of microfluidic channel was manufactured by the two-step-photolithography. Because of the SU-8 photoresist (SU-8 2015, MicroChem Corp, USA) consuming in the photolithography process [12], we obtained the extruded patterns on the wafer. We replicate the pattern on the wafer by using the PDMS. The PDMS microfluidic channel and nickel microstructure embedded PDMS thin layer are treated by the oxygen plasma (Plasma machine, Femto science, South Korea) and bond each other. To remain the stable bonding state, we cured the bonded structure on 100 °C. The channel on the device was treated with the pluronic solution (Pluronic F108 solution) on 12 hours to prevent the blood cells stick to the surface of channel. After pluronic solution treatment, we washed the channel with sterilized water. The syringe pump (Fusion 200, Chemyx, Inc., USA) was used for injecting the sample into the device and collecting the sample

from the outlet.

2.2 Magnetic nanoparticles conjugated with opsonin molecules

To capture the bacteria in the solution, we modified the magnetic nanoparticles with the opsonin molecule called human recombinant MBL[13]. MBL can bind many kinds of pathogens by recognizing the carbohydrate site of pathogen surface. The effective of MBL to capturing pathogens was already reported previous research[7]. We coated MBL on the surface of superparamagnetic nanoparticles (diameter: 200 nm) (Ademtech, France) which have streptavidin on the surface. At the first step, MBL (0.25 mg/mL) was biotinylated by incubating with biotinylation reagent (10×10^{-3} M) over 30 min at room temperature. The superparamagnetic nanoparticles (25 μg of MBL / mg of magnetic nanoparticles) were incubated with biotinylated MBL for 1 hour. Phosphate buffered saline including 1 % bovine serum was used to wash the magnetic nanoparticles. Before using for experiment, the MBL treated superparamagnetic nanoparticles were stored at 4 °C.

2.3 Capture efficiency of MBL conjugated superparamagnetic nanoparticles to bacteria

The MBL coated magnetic nanoparticles were tested the ability to binding bacteria E. coli. E. coli stock is prepared in 500 μL buffer solution ($CaCl_2$ (5×10^{-3} M), Tris (25×10^{-3} m), Tween 20 0.01%). The similar concentration (10^4 CFU/mL) of bacteria that we used for the test to evaluate the magnetic separation efficiency of our microfluidic chips was mixed with the MBL coated magnetic nanoparticles. To isolate bacteria bound with MBL coated magnetic nanoparticles, permanent magnet was placed for 3 min beside the tube containing the solution. And then the supernatant was transfer to the bacteria culture plate (LB agar plate) to evaluate the bacteria unbounded with MBL coated magnetic nanoparticles.

2.4 Magnetic separation efficiency of device

The magnetic separation efficiency of the device was estimated by comparing the bacteria *E. coli* concentration of solution extracted from inlet and outlet 1, respectively. When *E. coli* bound with MBL coated magnetic nanoparticles are injected into the inlet of device, the device isolated the *E. coli* and expelled the purified solution to the outlet 1. The isolation ability of magnetic separation device was

measured by the purity of solution from outlet 1 by culturing the solution at the bacteria culture plate (LB agar plate). After culturing the samples, the LB agar plate incubated in the 36 ºC incubator at overnight. We counted the number of colonies of bacteria on the plate to calculate the concentration of bacteria in samples. When $C_{o,\ in}$ is the concentration of *E. coli* in the inlet and $C_{o,\ out}$ is the concentrations of *E. coli* in the outlet 1 of magnetic separation device[10], the magnetic separation efficiency of the purposed device was addressed by

$$I_{mag} = \left(1 - \frac{C_{o,\ out}}{C_{o,\ in}}\right) \times 100$$

For the test of magnetic separation efficiency in blood, the blood sample was obtained from the rats (Healthy female Wistar, 8 weeks old). The collected blood stored in the blood collection tube (Vacutainer heparin tube, BD, Canada). Institutional Animal Care and Use Committee of Ulsan National Institute of Science and Technology (UNIST) proved the animal protocol. Results were expressed as mean of triplicate samples at least with standard deviations depicted by error bars in all graphs. Two tailed Student's t-test validate all data and $P<0.05$ were taken a statistically significant.

3. Results and discussion

3.1 Device design and fabrication

We designed the magnetophoretic separation microfluidic device, which induces chaotic advection flows. The device consists of one inlet where the sample is injected into the channel, two outlets where the sample flows out from the channel. A channel contains slanted micro ridge arrays and integrated with ferromagnetic nickel structure. Spiral flow can be formed by the asymmetric pressure gradients across the channel which is induced by the slanted micro ridge arrays[14](Figure 1A). The magnetic particles binding with target cells are transferred by the spiral flow and pass through the area with higher magnetic flux density gradients near the ferromagnetic structure (Figure 1B). When applying the external magnetic field using a permanent magnet, the nickel structure generates locally augmented magnetic flux density gradients and isolates magnetizable objects that pass near the ferromagnetic structure (Figure 2). The particles magnetically separated by the nickel structures followed the streamlines and then exited through the outlet 2 whereas the particle-depleted sample solution flow out through the outlet 1 (Figure 3 A).

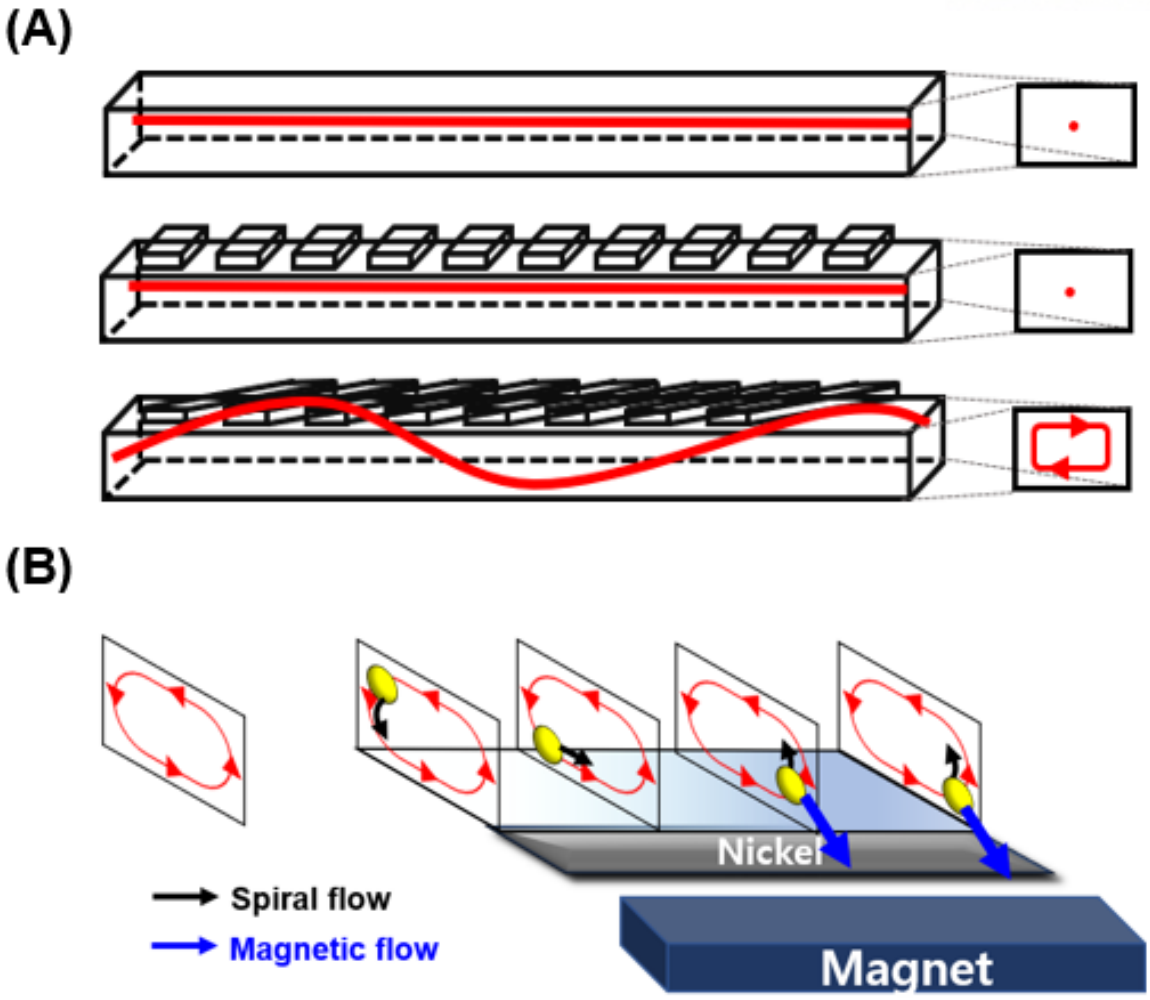

Figure 1. (A) The different streamlines induced by the shape of microgeometry in the channel. Slanted ridge arrays pattern induces the asymmetric pressure gradient and then generate the spiral flow in the channel. (B) The red arrows represent the rotational flows that can transfer the magnetic particles to the high magnetic forces formed area. The blue arrows represent the augmented magnetic force near the nickel structure. This high magnetic force rapidly isolated the magnetic particles.

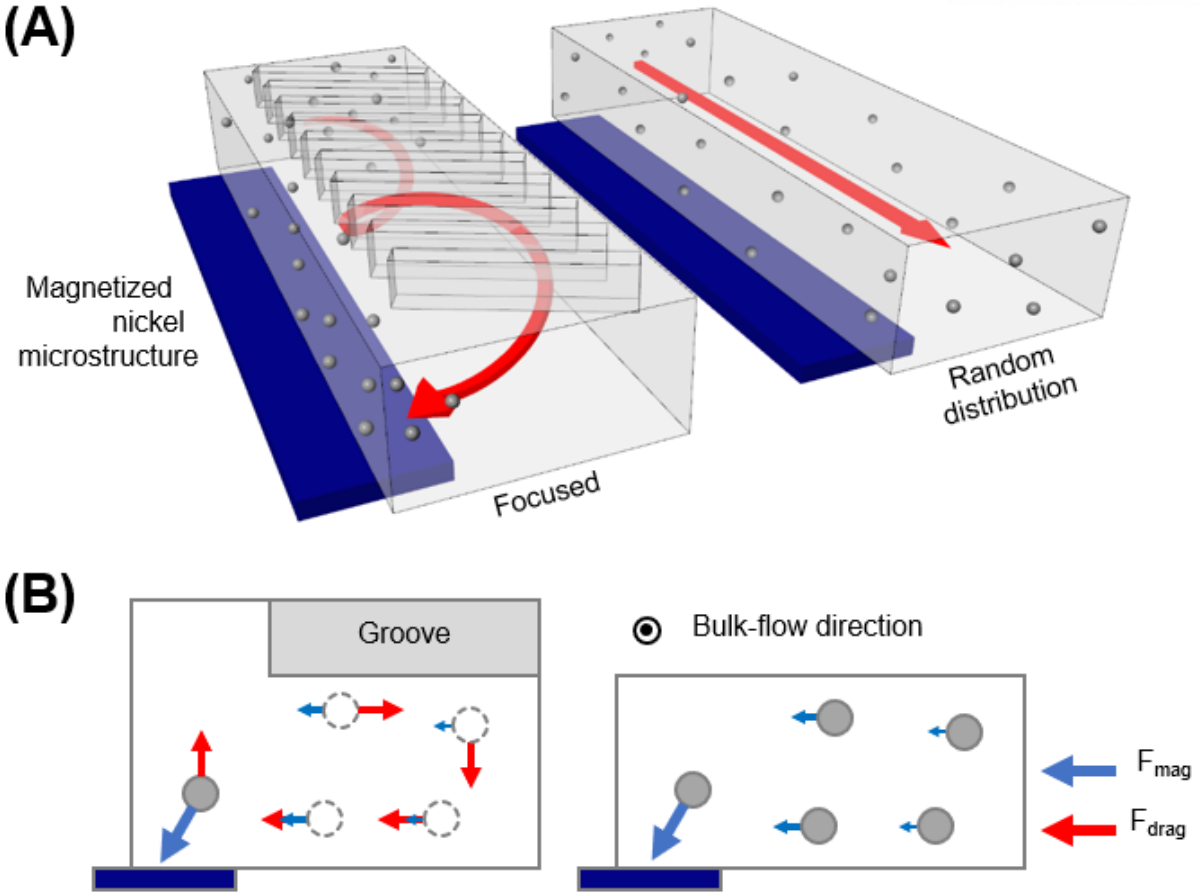

Figure 2. (A) A schematic view of the magnetic separation device that we proposed to improve the throughput of magnetic separation efficiency inducing spiral flow. (B) Cross-sectional schematic diagram of the magnetic separation device. When the magnetic particles that are transferred by the advective rotational flow meet the high magnetic flux density gradient area, because of the overwhelming magnetic drug velocity, the magnetic particles are isolated by the magnetic force.

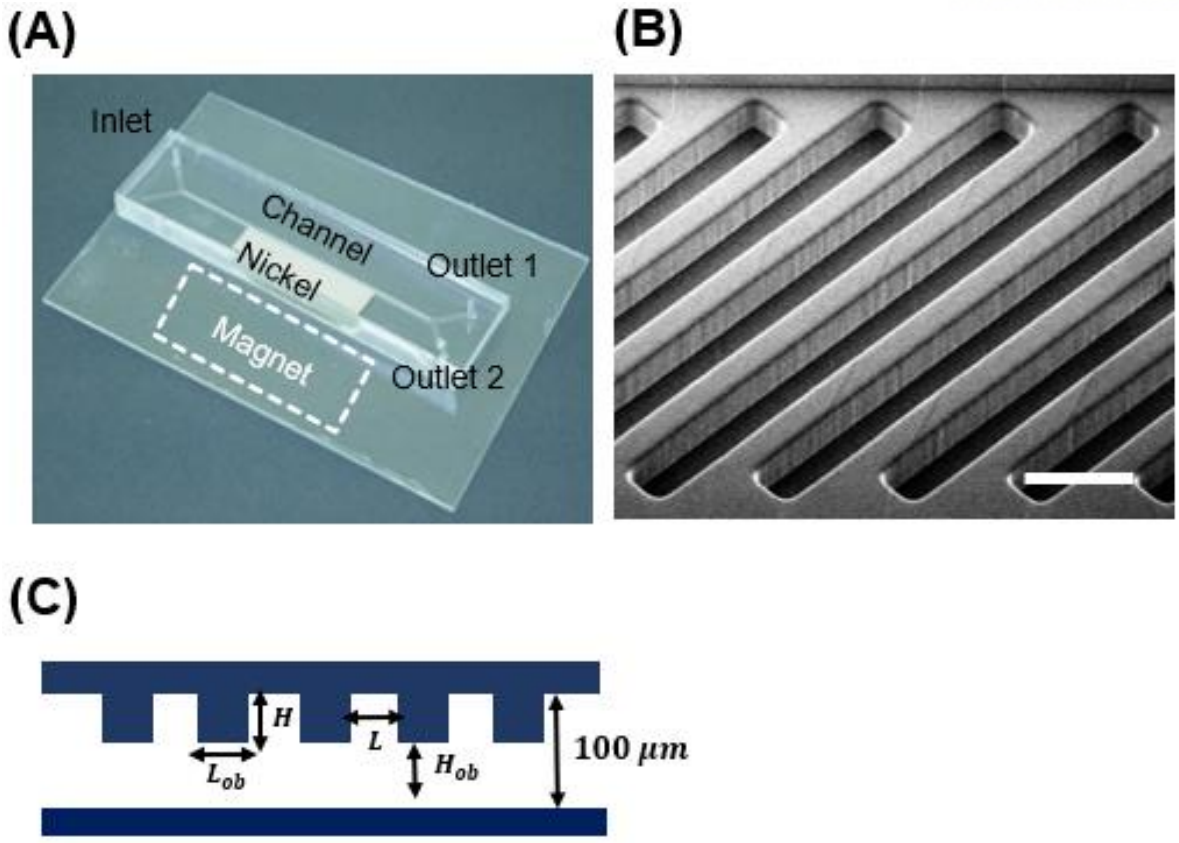

Figure 3. (A) Image of manufactured microfluidic device (B) Scanning electron microscope image of slanted ridge arrays integrated with the channel (Scale bar, 200 μm) (C) A cross-sectional view in a longitudinal direction of the device showing dimensions of 100 μm in height. The slanted ridges were constructed to have H_{ob} = 50 μm, L_{ob} = 60 μm, and L = 40 μm.

We fabricated the microfluidic device, which contained the obstacle-array patterns in the channel by using photolithography process. The magnetic separation channel (height of the channel × height of the ridge part in the channel × width of the channel; 100 μm × 50 μm × 1000 μm) was patterned the micro-obstacle arrays (Figure 3 B). The slanted obstacle structures were angled at 45 ° to generate sufficient rotational flows in the channel. Therefore, the channel with slanted ridge arrays generated spiral flows when the fluid passes through the microfluidic channel.

The nickel microstructure (length × width × thickness ; 2.4 cm × 0.5 cm × 100 μm) was embedded in the thin PDMS membrane (100 μm) deposited on a slide glass using a method described previously[2]. The augmented magnetic flux density gradients were formed in the area of the microfluidic channel adjacent to the nickel microstructure. A ferromagnetic nickel microstructure integrated in the device

generates the enhanced magnetic flux density gradients across the microfluidic channel. This composition of magnetic force yields high efficiency for isolation of target sample bound with magnetic beads.

3.2 Simulation about the spiral flow of theoretical model

To assure the advective rotational flows in the slanted obstacle arrays patterned channel, we used the computational fluid dynamics program (COMSOL v4.2, Comsol Inc, USA) (Figure 4). And we verified the spiral flow which was consistent with the previous reports that has been revealed the fluid phenomenon [11], [14]. The particles going through the microfluidic channel which contains perpendicular obstacle arrays along the flow direction reveal the movement in a parallel direction to the channel. Whereas the channel with slanted obstacle arrays induce the 8.17 ° angled streamline of particles going through the channel (Figure 4B). The angled streamline is shown as the part of spiral flows which is generated by the asymmetric pressure gradient formed in the continuous running fluid.

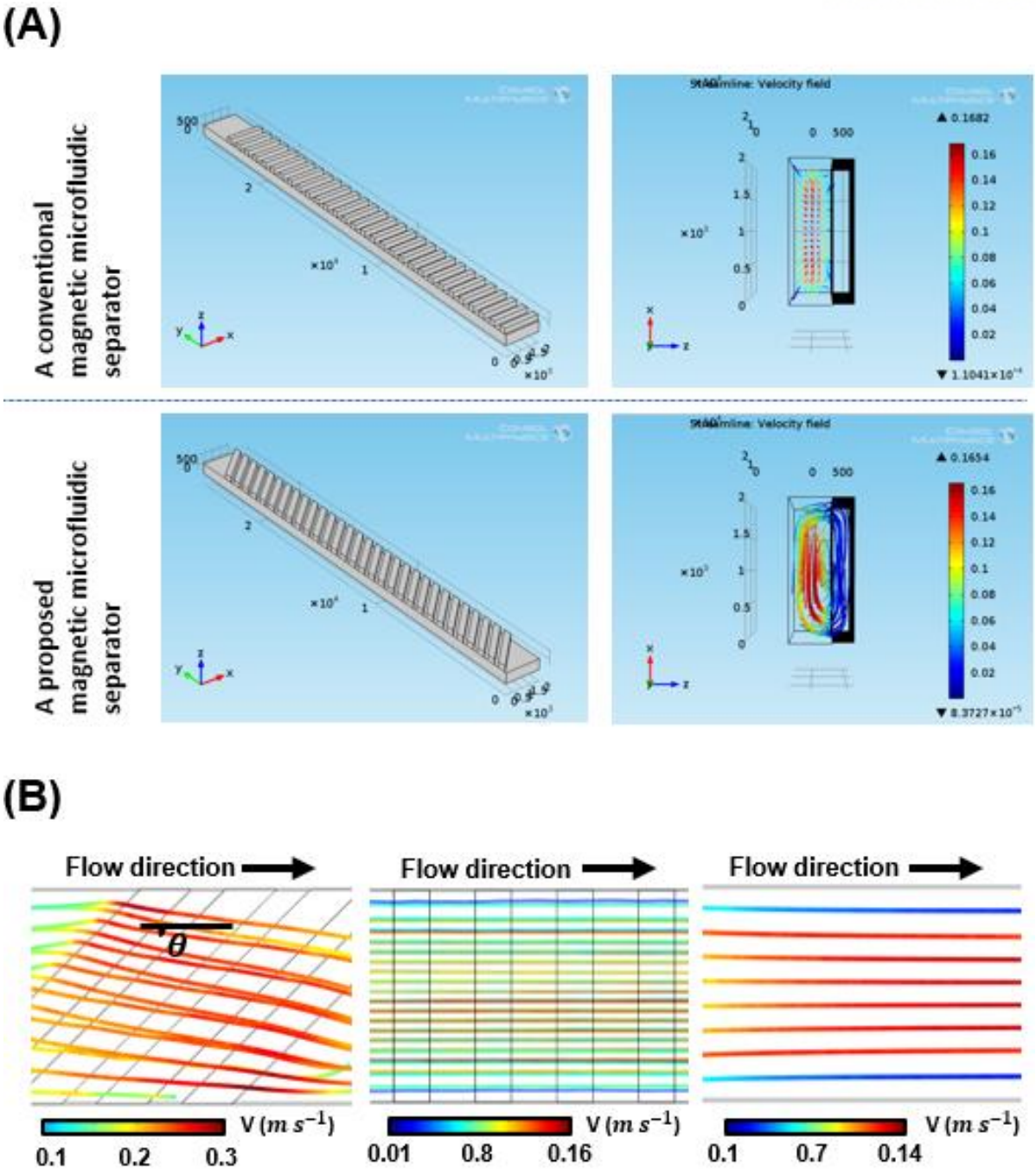

Figure 4. (A) The computational simulation geometry composed of non-slanted ridge (90 °) arrays (top) and slanted ridge (45 °) arrays (bottom). The spiral streamline is predicted at the slanted ridge arrays patterned channel. (B) COMSL software simulation results show top view images of the movement of particles. The angle θ = 8.17 ° along a side wall of the channel while other conventional channels were predicted parallel movement of particles along the side wall of the channel.

3.3 Simulation of improved magnetic separation in designed model.

We anticipated the trajectory of magnetic particles passing through the channel when the channel is exposed by the external magnetic force. By using the diverse formulas explaining fluid streamline, trace of particles and composition of magnetic force penetrating the channel, we revealed the computational simulation (MATLAB, The MathWorks, Inc, USA) result. The nickel structure adjacent to magnet generates the magnetic flux density gradients in the channel of microfluidic device. Finite element method magnetics software (FEMM) revealed the value of magnetic flux density gradients surrounding the nickel structure[2]. Compared to the state without nickel structure, the magnetic flux density gradients rapidly increase while getting closer to the nickel structure (Figure 5). The augmented magnetic force of the place adjacent to nickel structure was 7.68 μN while the side of channel far from the nickel structure was formed low magnetic force as 0.35 pN. Because of the extreme composition of magnetic flux density gradients near the nickel structure, the magnetic particles which are placed beyond 20 μm from the nickel structure are not attracted by the magnetic force. Where η is the dynamic viscosity of the surrounding solution, μ_0 is the vacuum permeability of the solution, R is a radius of a magnetic particle, χ_m is the magnetic susceptibility, B is the magnetic flux density, the magnetic drag velocity of magnetic particles (v) is addressed [15]

$$v = \frac{2\,R^2 \chi_m \nabla B^2}{9\eta\mu_0}$$

We perceived that the magnetic flux density gradients along the y-axis is equivalent at any position of x. In the case of no lateral advection flow, the lateral displacement of magnetic particle (d_{magnet}) dragging by magnetic forces at a time interval (t = 0.01s) can be obtained by

$$d_{magnet} = v \times t$$

, and the position of the particle can be defined as

$$x = \frac{Q}{a} \times t$$

$$y = v \times t$$

where Q is the flow rate of solution passing through the device, a is the area of cross sectional of microfluidic channel (width × height; 1000 μm × 40 μm). The magnetized nickel ferromagnetic structure generates the magnetic flux density gradients area which is dramatically decrease beyond 20 μm. Because of this formation of magnetic flux density gradients in microfluidic channel, the magnetic

particle going through the space in the channel far from the nickel structure cannot be entered the high magnetic flux density area. To position the magnetic particles from the low magnetic flux density area to high magnetic flux density area, we designed the slanted obstacle arrays patterned device where the particles are transferred by the spiral flow. The lateral displacement of magnetic particle was overwhelmingly determined by the advection rotational flow angled to head the nickel ferromagnetic structure. This streamline convinces the magnetic particle far from the nickel structure to move adjacent to the nickel structure. The displacement of magnetic particles in advective rotational flow ($d_{advection\ flow}$) can be defined as

$$d_{advection\ flow} = \frac{Q}{a} \times sin\,8.17\ \times t$$

When we exerted the external magnetic force, we defined the trajectory of magnetic particles as

$$d = d_{magnet} + d_{advection\ flow}$$

We assumed the velocity of magnetic particles in spiral flow as maximum rate which was revealed by the computer simulation program. At the maximum velocity $V_{advection\ flow\_max}$ apply for the position of magnetic particle in the y-axis

$$y = v \times t + V_{advection\ flow\_max} \times sin\,8.17\ \times t$$

The trajectory of magnetic particle plotted on figure 6 shown that the magnetic particles were transferred to the area adjacent to high magnetic flux gradient area (~20 μm) even they started at a distance of 660 μm away from the nickel structure.

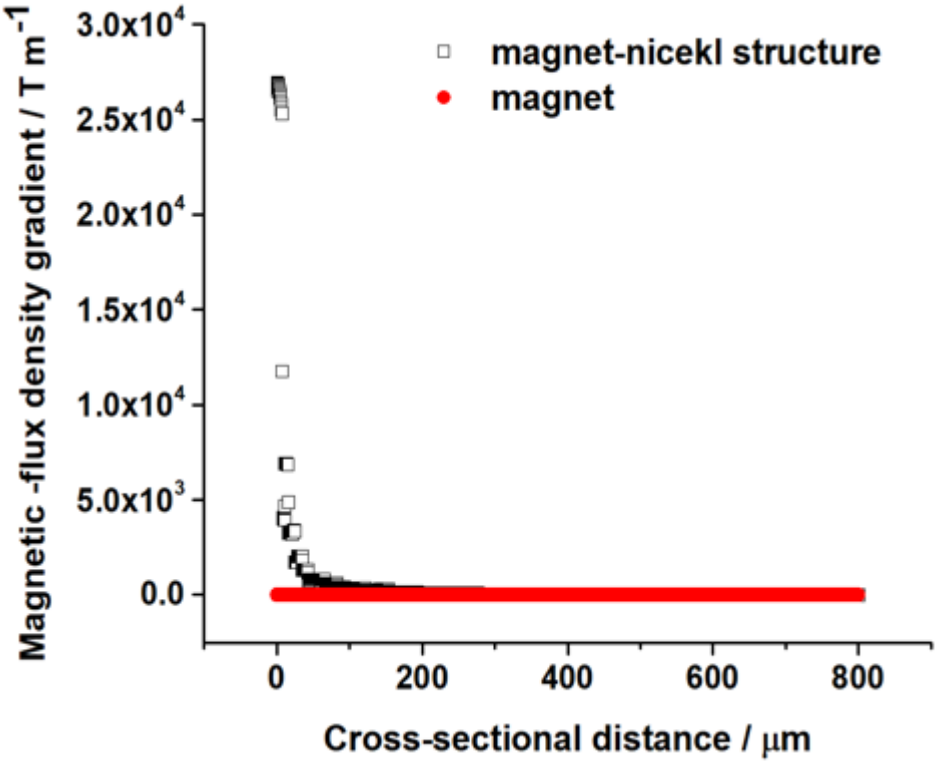

Figure 5. Plot of magnetic-flux density gradients along the distance from the nickel microstructure magnetized by a NdFeB permanent magnet

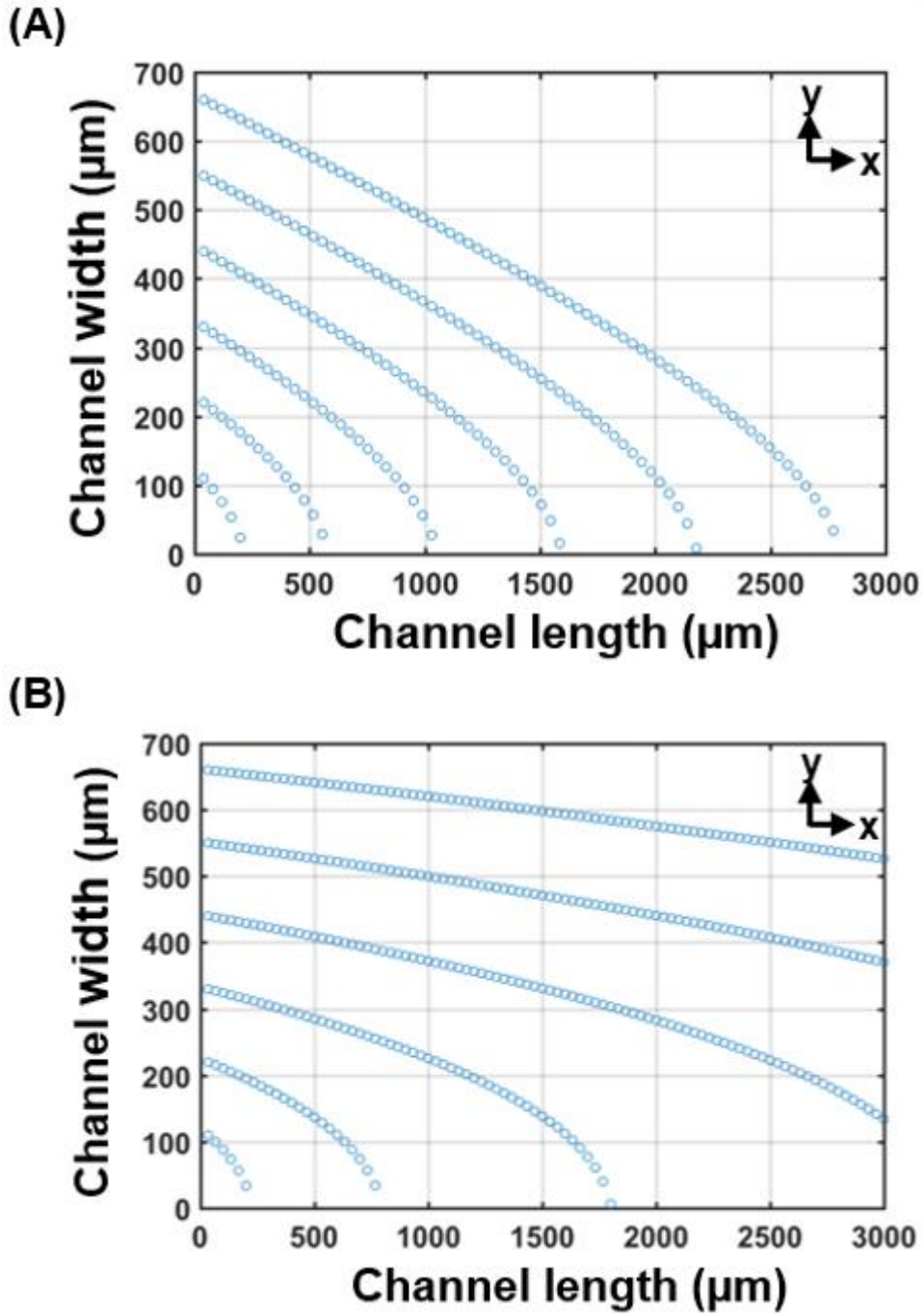

Figure 6. The computational simulation result of trajectories of magnetic particles going through the magnetic separation device integrated with (A) the slanted ridge arrays. And (B) the no-patterned flat channel, while being applied external magnetic force.

3.4 Advective rotational flow induce by slanted ridge arrays in channel.

To confirm the asymmetric pressure gradients formed by the slanted ridge arrays patterned channel, the solution contained fluorescent magnetic beads was injected into the device and we monitored the movement of magnetic beads. When the fluorescent paramagnetic particles injected in inlet as 2 μg/mL, the magnetic particle moved along the rotating stream induced by asymmetric pressure gradients, otherwise the 90 ° non-slanted obstacles generated parallel flow along the channel (Figure 7). We predicted the angled streamline (8.17 °) by using the computer simulation and this result equals with the movement of fluorescent magnetic beads. Because of the advective rotating flow in channel, the fluorescent magnetic beads movement formed streamline inclined to 8.58 ° at the top view of channel. However, other two designed channel with no spiral flow show the streamline appearing parallel direction to channel.

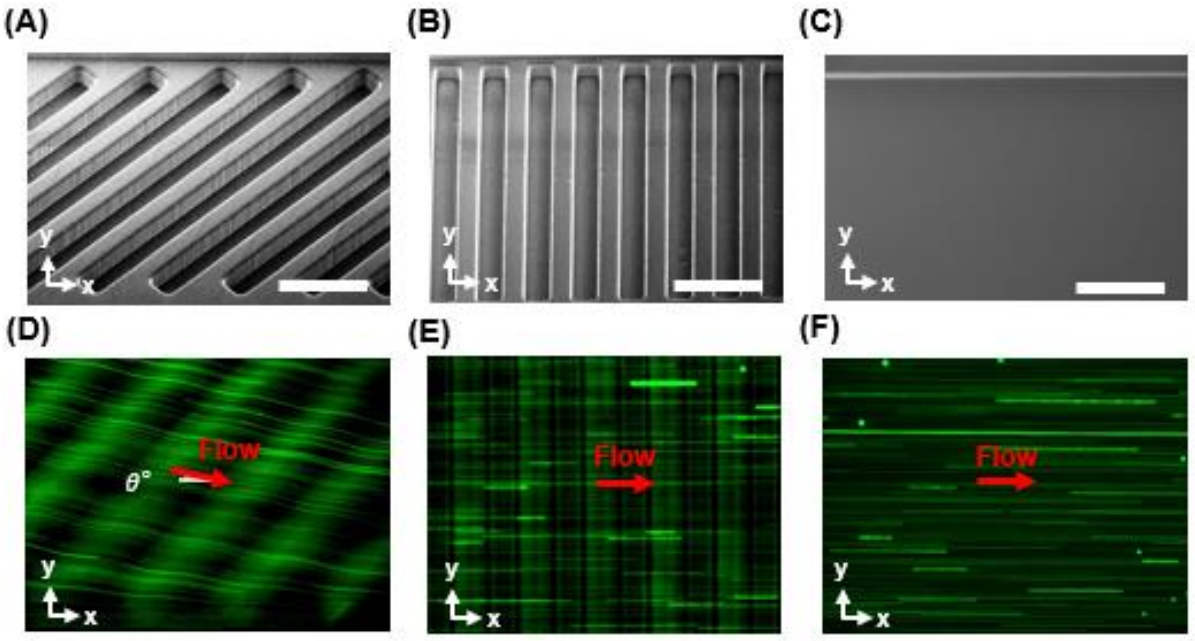

Figure 7. Traces of fluorescent magnetic particle (diameter: 1 μm) going through the microfluidic channels. (A), (B), (C) are the scanning electron microscope images that depict the micro-obstacles arrays 45 °, 90 °, and flat patterned on the channel, respectively. At the slanted ride arrays integrated channel demonstrates angled streamline (θ = 8.58 °) of particles induced by the spiral flow. This tilted angle is significantly similar with the computational simulation result.

3.5 Improved magnetic separation efficiency of magnetic particles

We validated our expectation about the magnetic separation efficiency using our designed microfluidic device (Figure 8). The embedded nickel ferromagnetic structure is magnetized by putting the permanent magnet nearby device[2]. To estimate the separation efficiency of our microfluidic device, we injected the 1 μm diameter of magnetic particle into the three different designed magnetic separation devices respectively. One of the designed magnetic separation devices is our purposed one which produce the spiral flow inside of the channel however the other devices which are containing flat (no obstacle arrays) channel and perpendicular obstacle arrays patterned channel do not induce spiral flow. The perpendicular obstacles are vertical direction to a flow direction and then those generate parallel streamline about channel. Two devices with no spiral flow were manufactured to compare the magnetic separation efficiency and to demonstrate superiority of our purposed design. Compared to conventional devices with no spiral flow, the purposed design inducing spiral flow demonstrated the highest isolation efficiency about magnetic beads (diameter: 1 μm) at a flow rate of 0.4 mL/hour. Moreover, the isolation efficiency of magnetic particle passing through other two magnetic separation device without no spiral flow gradually decreased as flow rate increase at an interval of 0.4 mL/hour. When the flow rate increased up to 1.6 mL/hour, the two devices with no spiral flow derived low isolation efficiency of magnetic particle 55.7 %. Whereas the microfluidic device with slanted obstacles arrays highly isolated magnetic beads with 95.5 % at a flow rate of 1.6 mL/hour which is applicable isolation efficiency for continuous magnetic separation device. This result is basically an extension of our prediction about magnetic bead movement in designed microfluidic device with external magnetic force. The spiral flow laterally transmigrated the magnetic beads repeatedly to the area of augmented magnetic force and then isolated promptly.

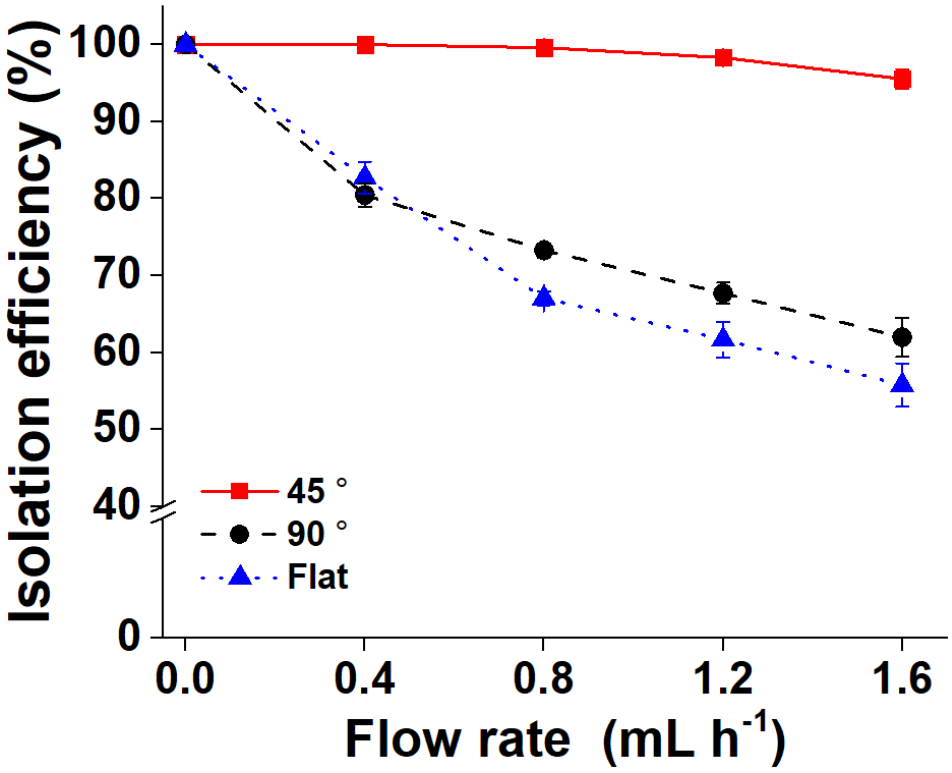

Figure 8. Isolation efficiency of magnetic particles (diameter: 1um) using microfluidic devices with different ridge angles and patterns. The flow rate gradually increases until 1.6 mL/hour

3.6 Isolation of Escherichia Coli captured by MBL-Magnetic Nanoparticles.

The ultimate goal of our design is to accomplish applicable magnetic separation device for separating biological targets from the variable types of solution. In this paper, we targeted bacteria and tried to isolating bacteria called *E. coli* form the solution. In the previous report, the smaller size magnetic particles are more effectively capturing bacteria because of the mobility. We used the superparamagnetic particles with a diameter of 200 nm to capture the *E. coli*. To bind the bacteria, we coated magnetic nanoparticle with mannose binding lectin (MBL) that recognize the carbohydrate site of bacteria and bound to the surface. The *E. coli* concentration in solution was 10^4 colony forming unit (CFU) / mL. MBL coated magnetic nanoparticles were injected into the solution including bacteria and bounded with bacteria. The capture efficiency between *E. coli* and magnetic nanoparticles were estimated as a prior test and over 99% of bacteria are bound with the magnetic nanoparticle successfully. The magnetic isolation efficiency of purposed magnetic separation device was measured by comparing the concentration of bacteria from inlet and outlet, respectively (Figure 9). Over 99.7% of E. coli are isolated form the buffer by using the magnetic separation device including slanted ridge arrays.

Otherwise, two other magnetic separation devices including 90 ° angled ride arrays and flat surface yielded low isolation efficiency 77.6% and 71.7%, respectively at a flow rate of 1.4 mL/hour.

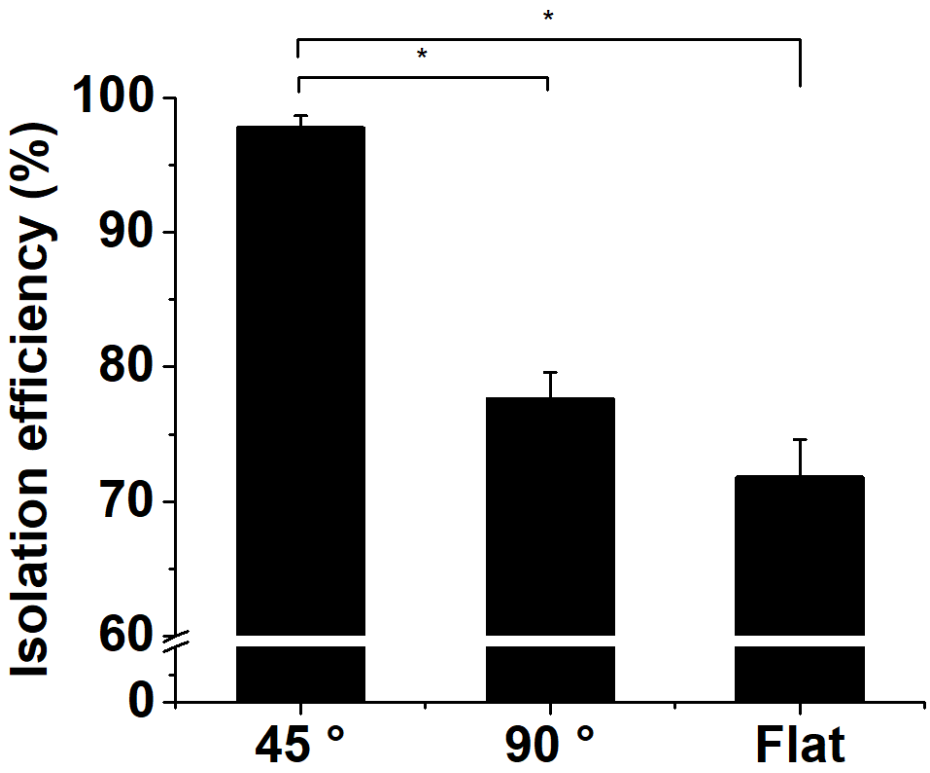

Figure 9. Isolation efficiency of E. coli bound with magnetic particle going through the magnetic separation devices integrated with different angles of ridge arrays at a flow rate of 1.4 mL/h (*, $P < 0.001$).

3.7 Isolation of Bacteria in diluted blood.

Because of the diverse components (erythrocyte, leukocyte, etc.) included in blood and high viscosity property, the blood is normally diluted for easily isolating targets. The concentration of targets in blood decreases because of the dilution process, therefore, high isolation efficiency of device becomes further emphasized. We validate the isolation efficiency of *E. coli* in 1:10 diluted blood by using our designed magnetic separation device (Figure 10). The microfluidic device inducing spiral flow isolated over 98% of *E. coli* from the diluted blood, while other conventional microfluidic device devices isolated under 25% of E. coli from the diluted blood.

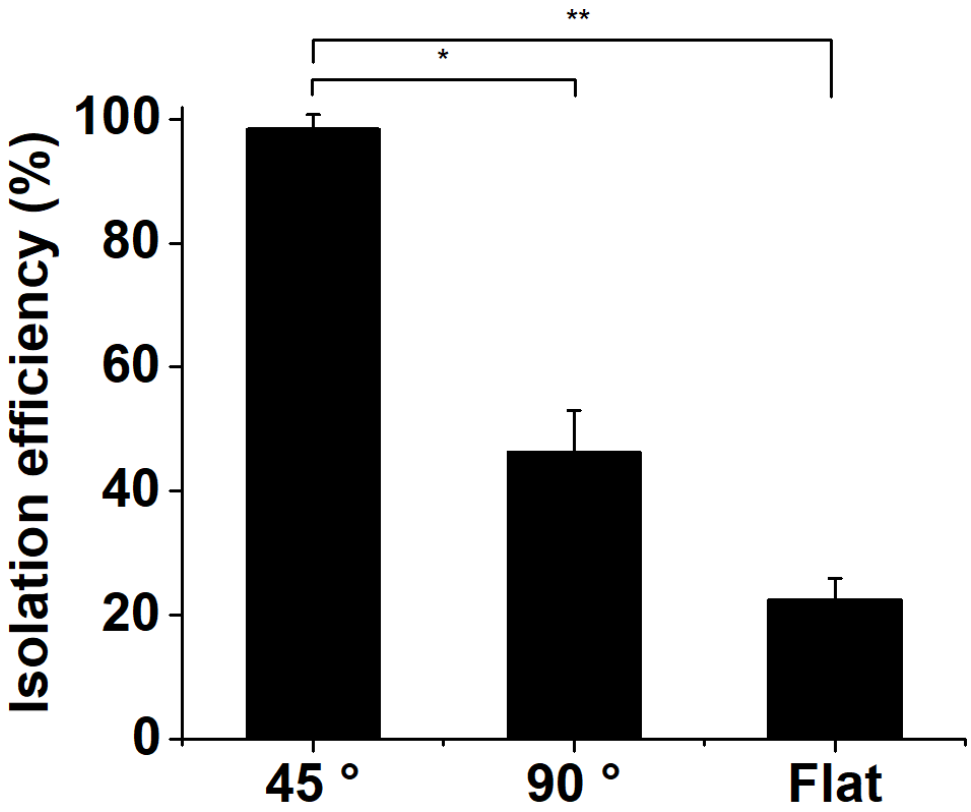

Figure 10. Isolation efficiency of E. coli bound with magnetic particles in diluted blood going through the magnetic separation devices integrated with different angles of ridge arrays at a flow rate of 1.4 mL/h. (*, $P < 0.001$; **, $P < 0.0001$)

3.8 Isolation of Bacteria in whole blood

In terms of clinical device, bacteria purifying efficiency from the whole blood is the key challenge for emergent therapy. *E. coli* prebound with the MBL coated magnetic nanoparticles was spiked into the whole blood. We injected bacteria contaminated whole blood into the slanted ridge arrays patterned magnetic separation device, and we verified 91.68% *E. coli* was isolated by the purposed device. Other two types of devices are isolated 27.72% and 23.95%, respectively (Figure 11). Due to the high viscosity of undiluted whole blood, the magnetic separation efficiency of two conventional devices became more decrease, while the spiral flow transferred the bacteria bound magnetic nanoparticles to augmented magnetic force area in our purposed design.

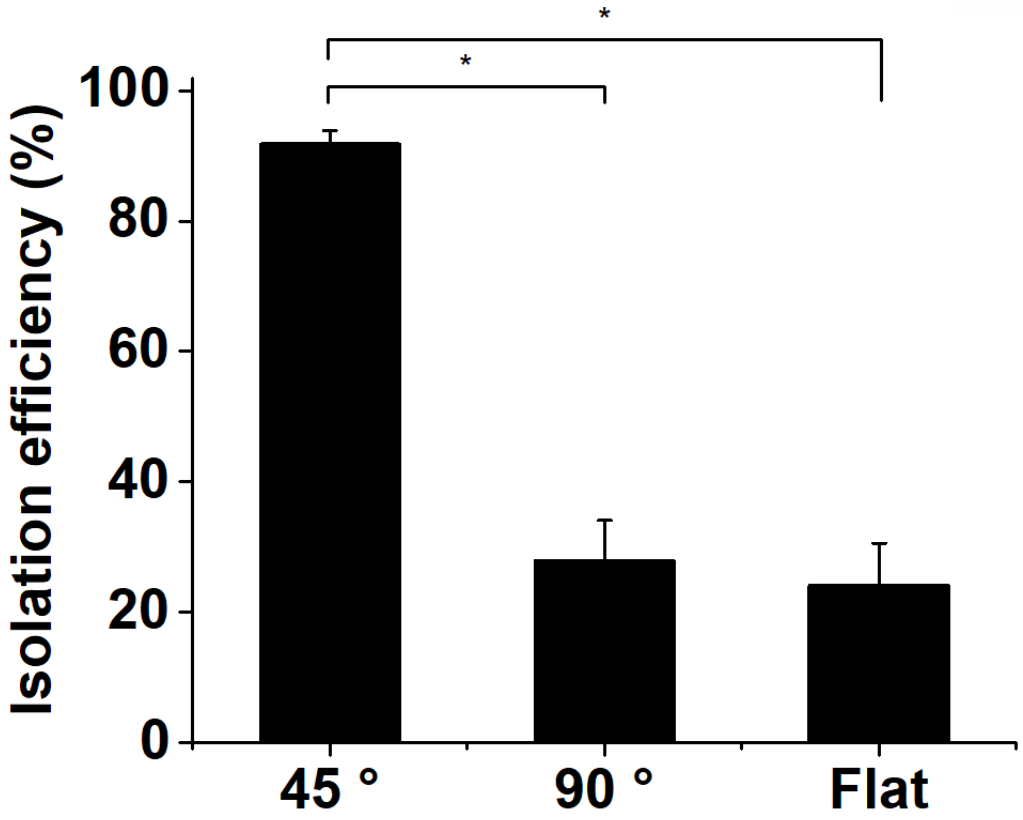

Figure 11. Isolation efficiency of E. coli bound with magnetic particles in whole blood going through the magnetic separation devices integrated with different angles of ridge arrays at a flow rate of 0.6 mL/h (*, $P < 0.001$).

4. Conclusion

We have proposed a magnetic separation device that uses advective rotational flows induced by patterned obstacles array on the wall of channel for the separation of micrometer particles. Many of the current continuous magnetic separation devices are limited to the separation of cells and micrometer sized biological molecules such as bacteria in blood sample remains a challenge because of the high viscosity. The use of rotational flows transfers the magnetic nanoparticles to the high augmented magnetic force area and then improves the magnetic separation efficiency overcoming the limitation. We theoretically predicted the superiority of the slanted ridge arrays integrated device for magnetic nanoparticles separation and then experimentally validated that our purposed device outperforms the spiral flows for isolating magnetic particles or magnetic nanoparticles bound bacteria. When applied to whole blood including *E. coli* bound magnetic particles, the slanted ridge arrays patterned device significantly purified the *E. coli* over 91.68% compared to < 27.72% removed using the conventional device that do not generate spiral flow. Our demonstration of the effectiveness of the spiral flow induced magnetic separation device provides an effective approach for high throughput magnetic separation that could be valuable for diverse applications, such as contaminated water purification[16], [17], food diagnostics[18], [19].

5. References

[1] O. Olsvik *et al.*, "Magnetic separation techniques in diagnostic microbiology.," *Clinical microbiology reviews*, vol. 7, no. 1, pp. 43–54, 1994.

[2] J. H. Kang and J.-K. Park, "Magnetophoretic Continuous Purification of Single-Walled Carbon Nanotubes from Catalytic Impurities in a Microfluidic Device," *Small*, vol. 3, no. 10, pp. 1784–1791, Oct. 2007.

[3] C. deLatour, G. Schmitz, E. Maxwell, and D. Kelland, "Designing HGMS matrix arrays for selective filtration," *IEEE Transactions on Magnetics*, vol. 19, no. 5, pp. 2127–2129, Sep. 1983.

[4] E. H. Dunlop, W. A. Feiler, and M. J. Mattione, "Magnetic separation in biotechnology," *Biotechnology advances*, vol. 2, no. 1, pp. 63–74, 1984.

[5] J. H. Kang, S. Krause, H. Tobin, A. Mammoto, M. Kanapathipillai, and D. E. Ingber, "A combined micromagnetic-microfluidic device for rapid capture and culture of rare circulating tumor cells," *Lab on a Chip*, vol. 12, no. 12, p. 2175, 2012.

[6] S. Berensmeier, "Magnetic particles for the separation and purification of nucleic acids," *Applied Microbiology and Biotechnology*, vol. 73, no. 3, pp. 495–504, Nov. 2006.

[7] J. H. Kang *et al.*, "An extracorporeal blood-cleansing device for sepsis therapy," *Nat. Med.*, vol. 20, no. 10, pp. 1211–1216, Oct. 2014.

[8] J.-J. Lee *et al.*, "Synthetic Ligand-Coated Magnetic Nanoparticles for Microfluidic Bacterial Separation from Blood," *Nano Letters*, vol. 14, no. 1, pp. 1–5, Jan. 2014.

[9] J. H. Kang, H. Driscoll, M. Super, and D. E. Ingber, "Application of a Halbach magnetic array for long-range cell and particle separations in biological samples," *Appl. Phys. Lett.*, vol. 108, no. 21, p. 213702, May 2016.

[10] J. H. Kang *et al.*, "Optimization of Pathogen Capture in Flowing Fluids with Magnetic Nanoparticles," *Small*, vol. 11, no. 42, pp. 5657–5666, Nov. 2015.

[11] S. Choi and J.-K. Park, "Continuous hydrophoretic separation and sizing of microparticles using slanted obstacles in a microchannel," *Lab on a Chip*, vol. 7, no. 7, p. 890, 2007.

[12] D. C. Duffy, J. C. McDonald, O. J. A. Schueller, and G. M. Whitesides, "Rapid Prototyping of Microfluidic Systems in Poly(dimethylsiloxane)," *Analytical Chemistry*, vol. 70, no. 23, pp. 4974–4984, Dec. 1998.

[13] R. M. Dommett, N. Klein, and M. W. Turner, "Mannose-binding lectin in innate immunity: past, present and future," *Tissue Antigens*, vol. 68, no. 3, pp. 193–209, Sep. 2006.

[14] A. D. Stroock, "Chaotic Mixer for Microchannels," *Science*, vol. 295, no. 5555, pp. 647–651, Jan. 2002.

[15] J. H. Kang, S. Choi, W. Lee, and J.-K. Park, "Isomagnetophoresis to Discriminate Subtle Difference in Magnetic Susceptibility," *Journal of the American Chemical Society*, vol. 130, no. 2, pp. 396–397, Jan. 2008.

[16] K. A. Shaikh *et al.*, “A modular microfluidic architecture for integrated biochemical analysis,” *Proceedings of the National Academy of Sciences*, vol. 102, no. 28, pp. 9745–9750, Jul. 2005.

[17] Q. Ramadan and M. A. M. Gijs, “Microfluidic applications of functionalized magnetic particles for environmental analysis: focus on waterborne pathogen detection,” *Microfluidics and Nanofluidics*, vol. 13, no. 4, pp. 529–542, Oct. 2012.

[18] J. Schemberg, A. Grodrian, R. RÃ¶mer, G. Gastrock, and K. Lemke, “Online optical detection of food contaminants in microdroplets,” *Engineering in Life Sciences*, vol. 9, no. 5, pp. 391–397, Oct. 2009.

[19] J.-Y. Yoon and B. Kim, “Lab-on-a-Chip Pathogen Sensors for Food Safety,” *Sensors*, vol. 12, no. 12, pp. 10713–10741, Aug. 2012.

6. Acknowledgement

I would like to express my special thanks my supervisor, Professor Joo Hun Kang who gave me the golden opportunity to do this project. I am grateful to him for his understanding, guidance, encouragement and insightful support in the whole process. I thank profusely all the members in our lab for their kind help and co-operation throughout my study period. I am also thankful Professor Young Ki Hahn, Sein Oh, Doctor Seyong Kwon, Professor Eujin Um and Professor Sungyoung Choi for their guidance and constant supervision.